Atmos. Chem. Phys. Discuss., 9, 27063–27098, 2009
www.atmos-chem-phys-discuss.net/9/27063/2009/

Atmospheric Chemistry and Physics Discussions

This discussion paper is/has been under review for the journal Atmospheric Chemistry and Physics (ACP). Please refer to the corresponding final paper in ACP if available.

Evaluation of a regional air quality forecast model for tropospheric NO_2 columns using the OMI/AURA satellite tropospheric NO_2 product

F. L. Herron-Thorpe, J. K. Vaughan, B. K. Lamb, and G. H. Mount

Laboratory for Atmospheric Research, Department of Civil & Environmental Engineering, Washington State University, Pullman, WA 99164-2910, USA

Received: 12 November 2009 – Accepted: 30 November 2009
– Published: 15 December 2009

Correspondence to: F. L. Herron-Thorpe (farrenthorpe@wsu.edu)

Published by Copernicus Publications on behalf of the European Geosciences Union.

Abstract

Results from a regional air quality forecast model, AIRPACT-3, are compared to OMI tropospheric NO_2 integrated column densities for an 18 month period over the Pacific Northwest. AIRPACT column densities were well correlated with cloud-free monthly averages of tropospheric NO_2 (R=0.75) to NASA retrievals for months without wildfires, but were poorly correlated with significant model overpredictions (R=0.21) for months with wildfires when OMI and AIRPACT were compared over the entire domain. AIRPACT forecasted higher NO_2 in some US urban areas, and lower NO_2 in many Canadian urban areas, when compared to OMI. There are significant changes in results after spatially averaging model results to the daily OMI swath. Also, it is shown that applying the averaging kernel to model results in cloudy conditions has a large effect, but applying the averaging kernel in cloud free conditions has little effect. The KNMI and NASA retrievals of tropospheric NO_2 from OMI (collection 3) are compared. The NASA product is shown to be significantly different than the KNMI tropospheric NO_2 product, i.e. July 2007 (R=0.60) and January 2008 (R=0.69).

1 Introduction

Nitrogen oxides (NO_x) are emitted into the atmosphere from natural sources, motor vehicles, and other combustion processes. NO_2 is controlled as a criteria pollutant which causes adverse health effects. NO_x acts as a chemical precursor to regional ozone, acid rain, and nitrate aerosol formation. NO_2 is an important part of urban atmospheric chemistry with large diurnal variations due to a strong dependence on mobile emissions and incident sunlight. In the past few decades, catalytic converters on automobiles have become more effective and have significantly reduced NO_x formation by catalytic reduction to O_2 and N_2. This has greatly reduced the emissions per vehicle, but regional ozone formation continues to be a problem. Studying regional air quality using Chemical Transport Models (CTMs) such as the Community Multi-scale

ACPD

9, 27063–27098, 2009

Air Quality (CMAQ) model (Byun and Schere, 2006) can bring a greater understanding of atmospheric processes to scientists, policy makers, regulatory agencies, and the community. Continuous monitoring of air quality provides a framework for evaluating model results and increasing model accuracy. In the Pacific Northwest, the density of surface air-quality monitors is sparse, especially for measuring NO_x. NASA's Earth Observing Satellites (EOS) provide air-quality researchers with a rich resource of daily global observations of our atmosphere, including tropospheric NO_2 column densities. Despite limitations of EOS spatial and temporal resolution, as compared to a regional CTM, afternoon column retrievals may prove useful for adjusting NO_x emissions inventories.

State agencies and the US EPA collectively provide a detailed emissions inventory by source and type that can be used to drive CTMs. Emissions processing by the Sparse Matrix Operator Kernel Emissions (SMOKE) modeling system and its companion programs such as MOBILE6 (EPA, 2003) utilize meteorological inputs to produce emissions estimates with a high degree of variation in time and space. The lifetime of NO_x is short, so the presence of high values in the troposphere are indicative of daily emissions, and discrepancies in a CTM's NO_x emission inventory should be evident when comparing satellite retrievals and model results for average daily NO_2. Emissions inventories for on-road vehicles have been particularly criticized (Parrish, 2006) and are difficult to predict given the variability of vehicle emissions. Recently, tropospheric NO_2 retrievals by satellite have been used to evaluate NO_x emission inventories used in CTMs through Kalman filter inversion (Napelenok, 2008). Assimilation through adjoint inverse modeling using 4-D-var algorithms have also been developed as described in Kurokawa et al. (2009) and Elbern et al. (2007).

Utilizing radiance properties and differential optical absorption spectroscopic (DOAS) techniques, satellite instruments can measure a slant column of NO_2 which is divided by the air mass factor to determine a total vertical column density. NO_2 is found in both the troposphere and stratosphere and so the total column derived includes contributions from both regions of the atmosphere. The contribution of stratospheric NO_2

ACPD
9, 27063–27098, 2009

can be deduced from a chemistry-transport model and subtracted from the retrieved total column, resulting in a tropospheric column. Currently the SCHIAMACY, GOME, GOME-2, and OMI satellite instruments retrieve tropospheric NO_2 using this type of technique; among these, the OMI has the best spatial resolution with pixels approximately 12 km×24 km at nadir in normal operational mode.

OMI (Ozone Monitoring Instrument) is a Dutch instrument flying on the AURA satellite launched by NASA in July 2004. Unique level 2 data products are created by each of the KNMI (Royal Dutch Meteorological Institute) and NASA science teams. Both agencies employ similar, but not identical, techniques for deducing tropospheric NO_2 column abundances; hence the retrieval results are not identical numerically. Currently, the 3rd collection of tropospheric NO_2 is available to users from both KNMI and NASA. The KNMI site gives users access to near real-time (NRT) data of Europe and North America which is available within a few hours of the satellite overpass. This is valuable to applications needing NRT data, but unfortunately the NRT product does not represent the best calculation provided in the official data collection.

1.1 Overall goals

For this analysis, we have chosen to use both the NASA data product and KNMI data product as sources of evaluation for the AIRPACT-3 regional air quality forecast system for tropospheric NO_2 over 18 months. The overall goals for this work are to improve our understanding of atmospheric chemistry in the Pacific Northwest and to evaluate and improve the AIRPACT-3 air quality forecast system. The objective of this paper is to examine the spatial and temporal distribution of NO_2 using OMI in comparison to AIRPACT-3. We analyzed the effect of spatial averaging and applying the OMI averaging kernel. AIRPACT-3 forecast results and both OMI (KNMI and NASA) tropospheric NO_2 retrievals were analyzed for long term trends. In the future, the results will be used to evaluate and modify the NO_x emission inventory used in the forecast system. Overall, incorporating NASA air quality data products with AIRPACT-3 forecasts will help to continue to provide the Pacific Northwest with a state-of-the-art decision support

system.

1.2 AIRPACT-3: Air Indicator Report for Public Access and Community Tracking v.3

AIRPACT-3 is an air quality forecast system for the Pacific Northwest reporting to the public daily via the web. The AIRPACT system combines air chemistry and meteorology using community modeling software including the Weather Research Forecast (WRF) meteorological model (used the Mesoscale Model 5 (MM5) prior to April 2008) the SMOKE processing system and the Community Multi-scale Air Quality Model (CMAQ). The governing equations of CMAQ can be found in Byun and Schere (2006), which describes the calculations for advection, diffusion, chemical reactions, photolysis, cloud mixing, aerosol dynamics, and deposition. The AIRPACT-3 domain is shown in Fig. 1 and uses 12 km×12 km grid cells (95×95) with 21 vertical layers increasing in layer thickness from the surface to the height of stratosphere-troposphere exchange. Further details describing AIRPACT-3 and recent evaluation results are given in Chen et al. (2008). The forecast results, along with automated evaluation results based upon AIRNOW monitoring data, are provided on a daily basis on the AIRPACT web site (http://www.lar.wsu.edu/airpact-3/).

The SMOKE tool is used to process anthropogenic emission categories for each forecast simulation. Area and non-road mobile emissions are based on the 2002 EPA NEI and adjusted using the EPA's Economic Growth Analysis System (EGAS) software. On-road mobile emissions are generated using emission factors from the EPA MOBILE v6.2 model and state specific activity data. Anthropogenic emissions over provinces of British Columbia and Alberta, Canada are included from the 2000 Greater Vancouver Regional District (GVRD) inventory. Fire emissions for the period of analysis were obtained from BlueSky (http://www.airfire.org/bluesky), utilizing ICS-209 reports and providing necessary inputs to SMOKE. More information about emissions processing in AIRPACT can be found in Chen et al. (2008).

ACPD
9, 27063–27098, 2009

1.3 OMI: Ozone Monitoring Instrument (http://aura.gsfc.nasa.gov/)

The Ozone Monitoring Instrument (OMI) is a Dutch instrument aboard the Aura satellite measuring daily global tropospheric and stratospheric chemistry of species such as NO_2, O_3, AOD, SO_2, and HCHO. Aura is in a sun-synchronous orbit (overpass time ~1:45 p.m.) and continually provides data for the "Afternoon-Train" of satellites. The analysis in this paper utilizes the OMI Level 2 NO_2 (Collection 3) where each orbit dataset is a 1644×60 grid, with 13 km×24 km footprint (at nadir), and covers approximately 1/14th of the globe with varying area and angle during each orbit. Operational level 2 data for OMI is generally available within 1.5 d after the satellite overpass and NASA data can be obtained from the Mirador service provided by the Goddard Space Flight Center (http://mirador.gsfc.nasa.gov) while KNMI data is available from the Tropospheric Emission Monitoring Internet Service (TEMIS) at http://www.temis.nl/airpollution/no2.html. The OMI Algorithm Theoretical Basis Document, Vol. 4 from NASA (Chance, 2002) discusses the specifics of trace gas retrievals, including NO_2.

The OMI NO_2 product is a useful data source for air-quality researchers, especially because it provides a daily tropospheric NO_2 vertical column density at resolutions useful for regional analyses. As discussed in Bucsela et al. (2006) satellite-based Earth radiance measurements yield trace gas columns, but require the use of radiative transfer models and a geo-referencing scheme to identify areas where there is commonly pollution in the boundary layer. This approach therefore involves use of some a priori information of spatial distribution of tropospheric and stratospheric NO_2. Validation efforts for the OMI NO_2 have shown that OMI is performing well and providing valuable information. For instance, during INTEX-B validation in Mexico (Boersma, 2008), a correlation of R=0.82 and slope=0.99 was found when OMI (NRT KNMI) was compared to airplane measurements. In the UK, correlation was found to be between R=0.64 and R=0.83, depending on season (Kramer, 2008), when OMI was compared to MAX-DOAS ground measurements.

2 Methods

Remote sensing by polar orbiting visible/UV satellite instruments involve a number of limitations when compared to a tropospheric air quality model. These include: 1) cloud cover that limits the depth of the retrieval as seen from space, 2) only one useful day-time data value is reliably obtained per geo-location, 3) horizontal resolution is generally not as fine as a regional model, and 4) the conversion of observed slant columns to a useful tropospheric column abundance is difficult. For these reasons, our analysis is only relevant for early afternoon abundances of tropospheric NO_2 during times of low cloud cover (<35%) for pixels not dominated by point sources. Our overall goal is to make future NO_x emissions adjustments based on previous OMI/AIRPACT comparisons. Utilizing temporal averaging is necessary for identifying biases in AIRPACT's NO_x emissions inventory, due to day-to-day variability. So, to avoid associated complications, we concentrated on averaging periods on a monthly basis throughout the entire year. These monthly averages are analyzed for the entire domain with a focus on biases in urban areas and some attention given to wildfire periods and locations. To properly evaluate the correlation between OMI and AIRPACT, we tested the effects of spatially averaging the AIRPACT grid to the daily OMI swaths. We also tested the effects of applying the OMI averaging kernel, which depends both on the measurement sensitivity and assumptions made for the retrieval. This helps account for assumptions made in the retrieval on the vertical distribution of NO_2 to make a consistent comparison between the modeled and measured columns (http://www.doas-bremen.de/doas_glossary.htm). An 18 month trend analysis from March 2007 to August 2008 was completed to compare OMI and AIRPACT tropospheric NO_2 columns within the AIRPACT domain.

2.1 Independent AIRPACT column derivation

For the period of analysis presented here, AIRPACT employed MM5 (http://www.mmm.ucar.edu/mm5) forecast fields provided by Mass and colleagues (Mass et al., 2003).

ACPD
9, 27063–27098, 2009

The meteorology forecasts are interpolated to the 21 layers used by AIRPACT, which uses the MCIP/SMOKE/CMAQ air quality modeling suite. The modeled domain horizontally spans 95×95 grid cells, with 12×12 km cells, and 21 vertical layers from the surface to approximately the tropopause height. Daily AIRPACT forecasts provide hourly averages of trace gases as mixing ratios, which must be integrated across all layers and converted to a "vertical column density" for direct comparison to tropospheric column density satellite retrievals. A vertical column density (VCD) can be calculated such that:

$$\mathrm{VCD} = \frac{m_{\mathrm{R}}(\mathrm{ppm})}{10^6} \cdot L_T(\mathrm{cm}) \cdot n_0(\mathrm{molecules/cm^3}) \quad (1)$$

where m_{R} is the mixing ratio of the trace gas, L_{T} is the model layer thickness, and n_0 is the number of total gas molecules per volume (Loschmidt's number). Loschmidt's number is dependent on temperature, pressure, and the gas constant such that:

$$n_0 = \frac{P}{R \cdot T} \quad (2)$$

Substituting in the definition of n_0 and summing across all 21 layers yields:

$$\mathrm{VCD} = \sum_{i=1}^{21} \frac{m_{Ri}}{10^6} \cdot \frac{L_{Ti} \cdot P_i \cdot N_A}{R \cdot T_i} \quad (3)$$

Accounting for units, and adjusting for available parameters and units from MCIP and CMAQ, we finally get:

$$\mathrm{VCD} = \sum_{i=1}^{21} m_{Ri} \cdot \frac{(\mathrm{ZF}_i - \mathrm{ZH}_i) \cdot \mathrm{PRES}_i}{\mathrm{TA}_i} \cdot 1.4486 \times 10^{13} \quad (4)$$

where VCD is the vertical column density in mol/cm^2, ZF is the layer full height in meters, ZH is the layer half height in meters, PRES is the layer pressure in pascals, and TA is the layer temperature average in Kelvins. This derivation of VCD from CMAQ and MCIP variables is independent of trace gas species type.

ACPD
9, 27063–27098, 2009

2.2 OMI tropospheric NO_2 column

After radiances have been collected, OMI Level 2 algorithms calculate a slant column density (SCD) of NO_2 that is divided by the calculated air mass factor (AMF) to yield a VCD for each pixel. The stratospheric contribution is dynamically determined with a planetary wave-2 model from the OMI data sampled in regions relatively free of tropospheric NO_2 (Eric Bucsela, private communication). Subtraction of the stratospheric contribution to the total column allows a tropospheric column residual to be calculated. A "below cloud" NO_2, or "ghost column", is estimated from global models and OMI's measurement of cloud cover pressure level. Summing the "below cloud" and "tropospheric" NO_2 gives the user a representation of a full column of NO_2 in the troposphere. However, it is important to keep in mind that the "below cloud" addition is not based on any current observation by the instrument. To account for this, our monthly average calculations are limited to using pixels with less than a 35% cloud fraction, where corresponding points from AIRPACT are masked from averaging as well.

The tropospheric columns that are calculated require the use of meteorological variables to calculate the number density of molecules throughout the atmosphere. This is quite simple for a model, as all variables can be exported and the user has a complete "state" of the atmosphere. However, OMI algorithms (Bucsela, 2006) use global model trends to determine average temperature and pressure on a coarse grid, and do not use current meteorological observations (or recent forecasts) to determine number density. This can be a relevant source of error when comparing model results to satellite derived columns.

2.3 The OMI averaging kernel and accounting for varied resolution

When comparing independent datasets (i.e. ground based measurements or model results) to trace gas satellite retrievals, an averaging kernel should be applied (Bucsela, 2008) to account for the a priori profile and meteorological assumptions made when calculating the air mass factor. We employed the OMI (NASA) averaging kernel

ACPD
9, 27063–27098, 2009

to provide consistency between observation and model. This method uses fewer independent variables, such as temperature profile assumptions, that can create errors in the interpreted columns. (Bucsela, 2008) This approach is numerically intensive because it requires many more variables, functions, and data space to be calculated. The overall data flow for these methods are summarized in Fig. 2. It may be difficult for users to acquire the averaging kernels for OMI NO_2 as they are not readily available in the NASA data product. This is sometimes common for satellite products as discussed by Eskes and Boersma (2003). However, the latest version of KNMI data includes the averaging kernels in the daily level 2 data files.

We have calculated a 1-month base case (July 2007) to determine the effects of using the averaging kernel vs. independent column integration. Vertical columns are based on a slant column measurement and air mass factor. The air mass factor is calculated by using modeled meteorological variables as well as geometry, terrain variables, cloud properties, and a modeled a priori NO_2 profile. The a priori NO_2 fractional abundance used by OMI algorithms are generated from annual global GEOS-CHEM results (Bucsela et al., 2006) shown in Fig. 3. The GEOS-CHEM results have a $2^{\circ}\times2.5^{\circ}$ horizontal resolution and are re-gridded to $2^{\circ}\times2^{\circ}$ for use in the OMI algorithms using a nearest neighbor approach, which is then used to calculate the OMI AMF and account for below cloud NO_2. IDL routines and lookup tables were provided by Eric Bucsela to compute and apply the averaging kernel. The OMI averaging kernel was applied to every afternoon AIRPACT NO_2 profile in July 2007. This essentially allowed theoretical "slant columns" to be calculated. Dividing the AIRPACT theoretical "slant column" by the OMI AMF gives a tropospheric column value that is more appropriate for comparison to OMI retrievals.

The independent AIRPACT columns presented in our analysis were calculated per layer, which was automated in the daily operational forecast and archived. This decreased the amount of disk space used by a factor of four since mixing ratios, layer heights, pressure, and temperature did not have to be saved independently. Originally this was considered a good process because neither the NASA or KNMI averaging ker-

ACPD
9, 27063–27098, 2009

nels were available at the time. In retrospect, it would have been advantageous to save all needed variables per layer so that it would be feasible to apply the averaging kernel over the entire 18 months, once they became available. Subsequently, all calculations using the averaging kernel required reprocessing of the AIRPACT system for the days of interest.

Computing AMFs and averaging kernels for the OMI (NASA) tropospheric NO_2 product requires the use of many different variables such as viewing and sun geometry, cloud properties, pressures, reflectivity, and radiances. These values all vary per OMI pixel. So, it is important to average the corresponding AIRPACT mixing ratios that fall within the spatial boundaries of each OMI pixel. Basically, this process requires the user to spatially average the model grid to that day's OMI swath. Despite the numerical intensity involved with applying the NASA averaging kernel, spatially averaging the model results to the daily OMI swath requires only a simple additional function in scripting as compared to independent comparisons. It is a useful and efficient method to adjust model results based on the variance in OMI footprint size throughout the swath. Subsequently, all AIRPACT results were spatially averaged to the daily OMI swath in our 18 month analysis.

2.4 Accounting for comparisons of dissimilar spatial grids

The OMI Level 2 data product has varying pixel orientation and size per geo-location. So, OMI retrievals cannot be readily compared to model results on a pixel per pixel basis. Comparing OMI retrievals to AIRPACT forecasts for the entire domain requires using a spatial interpolation scheme. We chose a latitudinally parallel grid and used a Lambert equal area projection that has a horizontal resolution that matches AIRPACT for all comparisons. Afternoon data values from AIRPACT and OMI were interpolated to this static grid, based on a Delaunay triangulation scheme. Scripting then allowed the calculation of domain biases, averages, and urban area timelines over an 18 month period.

ACPD
9, 27063–27098, 2009

3 Results and discussion

Our analysis focuses on three areas: 1) methods comparisons to determine the effect of spatial averaging and applying the averaging kernel, 2) long term biases in the AIRPACT forecast results that were observed when compared to both KNMI and NASA tropospheric NO_2 retrievals, and 3) long term trends in differences between the KNMI and NASA tropospheric NO_2 retrievals.

3.1 Methods comparison

Utilizing a variety of comparison criteria provides a better understanding of the resultant differences when model and satellite data are numerically interpreted. In this section, we will investigate how the correlation of tropospheric NO_2 from OMI and AIRPACT-3 changes in the domain after spatially averaging model results and applying the averaging kernel.

In general, spatially averaging decreases steep gradients near high concentration locations. This is directly related to the footprint size of the OMI pixels, which are coarser than the AIRPACT grid. This effect should be expected, because essentially the process is decreasing the resolution of AIRPACT, and "washes out" small locations of minima and maxima. Over 18 months, binning and averaging AIRPACT data to the individual OMI pixels increased the domain correlation between OMI (NASA) and AIRPACT by 2%. Independent AIRPACT results (a) and AIRPACT results spatially averaged to the OMI swath (b) are shown in Figs. 4 and 5 for two different monthly averages.

In order to decrease the number of sources of error, it is appropriate to apply the averaging kernel to AIRPACT results. This essentially takes the pressure and NO_2 mixing ratio values from AIRPACT and calculates what could be thought of as a theoretical slant column. Using the air mass factor calculated by OMI algorithms, a new tropospheric column value can then be calculated for the AIRPACT forecast results. The IDL routines provided to us calculate the number density of each layer without

ACPD
9, 27063–27098, 2009

temperature dependence. This sometimes leads to very large values if the product of the layer mixing ratio and pressure equals the layer above it.

We have computed the monthly average of AIRPACT for July 2007, using the averaging kernel, to determine if there are any significant differences in the resultant columns. Correlation with OMI results decreases from R=0.36 to R<0.01 when the averaging kernel is applied due to the erroneously large values, as discussed above. If we remove the erroneous data from the monthly timeline (using an arbitrary cut-off limit), and recalculate the monthly average, correlation with OMI increases to R=0.52. Overall, the same general trends are found in the modeled columns, and no significant changes in biases are found after applying the averaging kernel and taking a monthly average.

Figure 7 shows the Seattle metro area tropospheric column NO_2 for July 2007. We can see some important effects of spatially averaging AIRPACT data to the OMI swath and applying the averaging kernel in an urban area. Spatially averaging reduces the column density average, because the high peak value (commonly seen at city centers in AIRPACT forecasts) is essentially washed out to a coarser resolution. Also, the binned AIRPACT data is often close to values obtained after applying the averaging kernel, but deviates most during times of high cloud cover. Applying the averaging kernel often raises the calculated vertical column density during high cloud cover. This is directly related to a lower AMF that is calculated for the portion of the column over clouds.

For the July 2007 base case, there is a correlation of R=0.79 between the independent AIRPACT columns and the AIRPACT columns with averaging kernel applied; there is a correlation of R=0.88 between the spatially averaged columns and the columns with the averaging kernel applied. In general, the interpretation of bias trends changes much more when we spatially average AIRPACT results, as opposed to applying the averaging kernel and masking the erroneous data. In theory, the result of applying the averaging kernel is the best numerical comparison between AIRPACT and OMI. However, after spatial averaging, temporal averaging, and cloud masking, the numerical

ACPD
9, 27063–27098, 2009

effect of applying the averaging kernel over an entire domain is very subtle. Due to the significantly increased computational cost and disk space needed to carry all of the needed variables through the averaging kernel process, and the problem of creating erroneously large values, it is undesirable to calculate vertical columns from the model in this manner over a long term analysis. Consequently, the averaging kernel was not applied for the 18 month analysis. When making long term comparisons, the spatially averaged AIRPACT values give a better representation of what should be directly compared to OMI, and are a significant improvement over the original independent column calculations.

3.2 General differences between AIRPACT-3 and OMI tropospheric NO_2

Our 18 month analysis of OMI and AIRPACT tropospheric NO_2 provided a significant source for evaluating AIRPACT results. In this section we will discuss the areas in our model domain that show a significant bias from both the NASA and KNMI OMI L2 Tropospheric NO_2 retrievals. AIRPACT predicts higher values in Seattle and lower values in Vancouver, B.C. during the summer. Correlation over the entire domain and trends in specific areas are summarized on a monthly basis in Table 1. Overall, AIRPACT is significantly better correlated to NASA retrievals than to KNMI retrievals. However, current AIRPACT predictions of NO_2 due to emissions from summer wild fires are significantly higher than retrievals by OMI (as well as carbon monoxide retrievals by AIRS – not shown). It has been discussed at OMI science teem meetings that OMI cannot get a reasonable measurement of boundary layer NO_2 in fire areas, due to the increased smoke/cloud cover. It is evident that correlation is drastically reduced during summer months where wildfires influence emissions in the domain. However, AIRPACT fire emissions for these forecasts used a less reliable method than current BlueSky technologies, as mentioned previously.

Figure 4 shows the many fire hot spots that AIRPACT forecasted with high NO_2 emissions during summer wildfires of July 2007. Notice the fires in South Oregon, Central Idaho, and Montana. For comparison, Fig. 5 shows January 2008, when there were no

ACPD
9, 27063–27098, 2009

recorded wildfires and emissions are largely from anthropogenic sources. Also, we see that column NO_2 in wildfire areas have a very large discrepancy and in fact AIRPACT is an order of magnitude higher than OMI over a monthly average. Investigation into the daily variation in NO_2 columns over wildfire areas has shown that OMI to AIRPACT ratios over wildfire areas can vary from 0.05 to 10. However, fire emissions were consistently propagated in AIRPACT at very high estimates for the entire fire season. This is in contrast to the slow periodicity of high NO_2 values retrieved by OMI over recorded fires. Ultimately, the AIRPACT averages included many more "reported" days.

In Boersma (2008), near real-time OMI data was used to determine top-down surface NO_x emissions for March 2006 over the contiguous United States and Mexico. The results were compared to bottom-up inventories for the INTEX-B domain by the US and Mexico Environmental Protection Agencies (US 1999 National Emission Inventory, NEI99). Emissions of NO_x were shown to be too high in the United States while Mexican emissions were too low. The analysis showed that for the US EPA NEI99 inventory point source NO_x emissions should be lowered and mobile emissions increased. This agrees with Kim et al. (2009) where a comparison of WRF-CHEM model results to satellite data showed their model to be ~10% higher for tropospheric columns over power plants. Our results with AIRPACT, though largely based on EPA's 2002 NEI, bring us to similar conclusions about the biases of NO_x emissions inventories used in urban areas when comparing Canada and the United States.

Vancouver, B.C. shows very good correlation for the months of January through June. However, July through December shows much higher OMI values and a strong bias that peaks at approximately 9×10^{15} molecules/cm^2 during the month of August (NASA). Vancouver B.C. shows a large OMI signal during the summer and late fall which is not generated with the current AIRPACT emissions inventory. In fact, emissions for Victoria (Vancouver Island, B.C., Canada) and urban areas south of Calgary, Canada could also be raised, given the comparisons to AIRPACT. These discrepancies could be due to an older emissions scenario from Canadian inventories. However, the fact that Victoria and Vancouver, B.C. share the same GEOS-CHEM a priori pixel as

ACPD
9, 27063–27098, 2009

Seattle raises some concern about the validity of this finding.

The 18 month urban area monthly averages for all three data sources and their spatial variation are graphed for 5 major urban areas: Portland, Oregon (Fig. 8); Boise, Idaho (Fig. 9); Vancouver, B.C. (Fig. 10); Salt Lake City, Utah (Fig. 11); and Seattle, Washington (Fig. 12). Generally, AIRPACT is between the range of NASA and KNMI retrievals in Salt Lake City, Boise, and Portland. However, AIRPACT's forcasts of Seattle NO_2 columns are generally higher than OMI retrievals.

3.3 Differences in NASA and KNMI datasets

Over 18 months, an average correlation of R=0.68 was calculated between the two OMI tropospheric NO_2 datasets. There was generally correlation above R=0.7, but two months with considerable noisy (striped) data decreased the correlation considerably. In fact, the KNMI datasets include negative values which often replace areas of striping and can significantly dominate some pixels when calculating a monthly average. This decreases correlation to NASA, as the NASA algorithm does not produce negative values. Table 2 shows the month-to-month correlation of KNMI to NASA datasets over the entire AIRPACT domain with commentary on overall trends.

It is important to note that the current collection 3 of OMI tropospheric NO_2 provided by NASA seems to cause a systematic trend of higher values in the summer. Stratospheric NO_2 is highest in the mid-latitudes during the summer (Cohen et al., 2003) which leads to a larger tropospheric residual for those months. Background levels of tropospheric NO_2 calculated by NASA are lower over the domain during the winter. However, all long-term NASA timelines show a clear anti-correlation with season. NASA values are higher in the summer, and lower in the winter, which is evidently due to the way that the tropospheric column is calculated in the OMI NO_2 algorithms. This cyclic variance in tropospheric NO_2 is not "real", but rather an artifact of the known issues with the OMI NO_2 stratosphere (not provided explicitly in the NASA product). Eric Bucsela (private communication) has identified these issues as: 1) the small amounts of tropospheric contamination in the data used to derive the stratosphere, 2) failure

to account for the diurnal cross-track variation of the stratosphere, and 3) issues introduced in the wave-2 interpolation. Also, the stratospheric AMF is also determined from an annual mean profile, but this has a relatively small effect. Wave-2 interpolation issues include the shapes of continents in the masked regions and the potential to hide planetary-scale structure in the troposphere (i.e. from lightning NO_x) and small-scale structure in the stratosphere.

The tropospheric NO_2 datasets provided by KNMI/TEMIS do not show the strong seasonal variation in the datasets that NASA retrievals do. This may be due to the fact that KNMI captures diurnal cross-track variation and small scale structures in the stratosphere not picked up by wave-2 interpolation (Bucsela, private communication). In fact, long-term KNMI trends seem to contrast the cyclical NASA trend, but the effect is not as clearly defined as the trend in NASA values. KNMI values for Salt Lake City are very large during winter months, while Portland values are quite small during summer months. Also, KNMI values over Vancouver are largest in the fall and winter as opposed to NASA's large summer values. In fact, nearly all urban KNMI averages were largest in cooler months. However, this effect may be expected naturally: less sunlight is incident on the airshed during cloud covered cool months, so less NO_2 is photolyzed to NO.

3.4 Future emissions corrections

Using long term averages of the OMI to AIRPACT ratio, simple emissions adjustment scenarios have been calculated for our July 2007 base case. As expected, "pulling" all emissions towards the average of satellite retrievals increases the average correlation with OMI over the domain, but this is an arbitrary result. An emissions adjustment used for air quality forecasting should address specific sources, so that the model can remain independently valid. However, it is difficult to properly adjust all emission source types based on NO_2 satellite retrievals, for the following reasons: 1) the emissions from individual point sources are not well resolved by DOAS satellite retrievals, 2) biogenic and area NO_x emissions are generally at a level below the detection limit of OMI, 3)

ACPD
9, 27063–27098, 2009

wildfire emissions would require a 4-D-var analysis using near real-time NO_2 retrievals for AIRPACT forecasting, which is outside the scope of this analysis, and 4) DOAS satellite retrievals do not readily resolve boundary layer concentrations.

Future work will target monthly NO_x emissions from mobile sources within the AIRPACT domain. Calculations have shown us that many parts of the domain are dominated by mobile NO_x, which will be targeted for adjustment based on the OMI/AIRPACT analyses. An inverse modeling scheme will help us create an optimized mobile NO_x emissions adjustment that can be used in operational forecasts. Zhao et al. (2009) describes the development of an optimized emissions inventory of fossil fuel NO_x using assimilated inversions on a daily basis, allowing for iterative adjustments, as opposed to one single inversion in a monthly-mean approach. That study found an increase in spatial covariance from 0.7–0.8 to 0.92 when using daily iterative inversions. However, the question remains as to which dataset should be used when adjusting emissions based on the OMI tropospheric NO_2 product. Ultimately, we have decided it would be best to make adjustments based on the average of the two data sets.

4 Conclusions and future work

Although there are sources of error in the OMI retrieval of NO_2, and limiting factors such as cloud cover, it is a rich source of data for evaluating a CTM over a long term period. Computing monthly averages of NO_2 in relatively cloud free conditions provided a significant database for evaluating the AIRPACT NO_x forecast levels. There are minor problems when comparing tropospheric NO_2 columns, such as stratospheric NO_2 abundances and a priori assumptions. However, long term trends in biases between OMI and a CTM can give researchers a definitive source to evaluate modeled NO_x in the troposphere for an entire modeling domain. This is a valuable source of validation in areas with a limited number of ground based NO_x monitors, as is the case in the Pacific Northwest.

Applying the OMI averaging kernel to the model results has the largest effect in

ACPD
9, 27063–27098, 2009

cloudy pixels and provides a comparison with the least possible introduced error. Applying the averaging kernel for cloud free conditions has very little effect on the modeled columns. Also, it is computationally expensive and can lead to erroneously large values when integrating the modeled column. Nevertheless, it is very important to spatially average all model results to the OMI swath. This helps to account for differences in resolution so as not to lead to inappropriate conclusions, particularly where there are strong point source emissions.

In our 18 month analysis of tropospheric NO_2 in the Pacific Northwest, we found a significant number of trends in both the OMI data and its relation to regional forecasts by AIRPACT. First of all, there is a seasonal effect of OMI tropospheric NO_2 from NASA, where high values are reported in the summer and low values in the winter. This is presumably a systematic outcome due to assumptions in the NASA algorithms and the seasonal variations in stratospheric NO_2. Despite this problem, we can clearly see that AIRPACT tends to underestimate in Canadian urban areas and sometimes overestimate in USA urban areas. This may be due to discrepancies in the way that emissions inventories are calculated in these two countries.

There are important implications of modeled ozone performance given these consistent biases. The urban areas in the domain are consistently VOC limited and so we would expect predicted ozone in Seattle to increase after an emissions adjustment, while it would decrease in Canadian cities such as Vancouver and Victoria. Another important finding is that AIRPACT predictions of summer wild fire emissions are nearly an order of magnitude higher than OMI retrievals over a monthly average. We look forward to working with the new BlueSky framework for processing wildfire emissions which should help to minimize error in wildfire locations and radiant energy. Finally, work is being done to increase AIRPACT forecast accuracy by adjusting mobile emissions based on an inverse modeling scheme. This will aim to increase OMI to AIRPACT tropospheric NO_2 correlations by adjusting mobile emissions sectors within the model.

Acknowledgement. This research was made possible by a grant from NASA for the North-West-AIRQUEST Decision Support System (grant #NNA06CN04A). The authors would like to

thank E. Bucsela as well as OMI team members from KNMI and NASA for their support in this project.

References

Blond, N., Boersma, K. F., Eskes, H. J., van der A, R. J., Roozendael, M. V., Smedt, I. D., Bergametti, G., and Vautard, R.: Intercomparison of SCHIAMACY nitrogen dioxide observations, in situ measurements and air quality modeling results over Western Europe, J. Geophys. Res., 112, D10311, doi:10.1029/2006JD007277, 2007.

Boersma, K. F., Eskes, H. J., and Brinksma, E. J.: Error analysis for tropospheric NO_2 retrieval from space, J. Geophys. Res., 109, D04311, doi:10.1029/2003JD003962, 2004.

Boersma, K. F., Jacob, D. J., Bucsela, E. J., Perring, A. E., Dirksen, R., van der A, R. J., Yantosca, R. M., Park, R. J., Wenig, M. O., Bertram, T. H., and Cohen, R. C.: Validation of OMI tropospheric NO_2 observations during INTEX-B and application to constrain NO_x emissions over the eastern United States and Mexico, Atmos. Environ., 42, 4480–4497, 2008.

Bucsela, E. J., Celarier, E. A., Wenig, M. O., Gleason, J. F., Veefkind, J. P., Boersma, K. F., and Brinksma, E. J.: Algorithm for NO_2 vertical column retrieval from the ozone monitoring instrument, IEEE T. Geosci. Remote, 44(5), 1245–1258, 2006.

Bucsela, E. J., Perring, A. E., Cohen, R. C., et al.: Comparison of tropospheric NO_2 from in situ aircraft measurements with near-real-time and standard product data from OMI, J. Geophys. Res., 113, D16S31, doi:10.1029/2007JD008838, 2008.

Byun, D. and Schere, K. L.: Review of the governing equations, computational algorithms, and other components of the models-3 community multiscale air quality (CMAQ) modeling system, Appl. Mech. Rev., 59, 51–77, 2006.

Chance, K.: OMI Algorithm Theoretical Basis Document, Vol. 4, OMI Trace Gas Algorithms, Smithsonian Astrophysical Observatory, 2002, http://eospso.gsfc.nasa.gov/eos_homepage/for_scientists/atbd/docs/OMI/ATBD-OMI-04.pdf.

Chen, J., Vaughan, J., Avise, J., O'Neill, S., and Lamb, B.: Enhancement and evaluation of the AIRPACT ozone and $PM_{2.5}$ forecast system for the Pacific Northwest, J. Geophys. Res., 113, D14305, doi:10.1029/2007JD009554, 2008.

Cohen, C. and Murphy, J.: Photochemistry of NO_2 in Earth's stratosphere: constraints from observations, Chem. Rev., 103(12), 4985–4998, doi:10.1021/cr020647x, 2003.
Elbern, H., Strunk, A., Schmidt, H., and Talagrand, O.: Emission rate and chemical state estimation by 4-dimensional variational inversion, Atmos. Chem. Phys., 7, 3749–3769, 2007, http://www.atmos-chem-phys.net/7/3749/2007/.
EPA: User's Guide to MOBILE 6.1 and 6.2: Mobile Source Emission Factor Model. EPA420-R-03-010, US Environmental Protection Agency, August 2003.
Eskes, H. J. and Boersma, K. F.: Averaging kernels for DOAS total-column satellite retrievals, Atmos. Chem. Phys., 3, 1285–1291, 2003, http://www.atmos-chem-phys.net/3/1285/2003/.
Kaynak, B., Hu, Y., Martin, R. V., Sioris, C. E., and Russell, A. G.: Comparison of weekly cycle of NO_2 satellite retrievals and NO_x emission inventories for the continental United States, J. Geophys. Res., 114, D05302, doi:10.1029/2008JD010714, 2009.
Kim, S.-W., Heckel, A., Frost, G. J., Richter, A., Gleason, J., Burrows, J. P., McKeen, S., Hsie, E.-Y., Granier, C., and Trainer, M.: NO_2 columns in the western United States observed from space and simulated by a regional chemistry model and their implications for NO_x emissions, J. Geophys. Res., 114, D11301, doi:10.1029/2008JD011343, 2009.
Kramer, L. J., Leigh, R. J., Remedios, J. J., and Monks, P. S.: Comparison of OMI and ground-based in situ and MAX-DOAS measurements of tropospheric nitrogen dioxide in an urban area, J. Geophys. Res., 113, D16S39, doi:10.1029/2007JD009168, 2008.
Kurokawa, J., Yumimoto, K., Uno, I., and Ohara, T.: Adjoint inverse modeling of NO_x emissions over eastern China using satellite observations of NO_2 vertical column densities, Atmos. Environ., 43, 1878–1887, 2009.
Mass, C. F., Albright, M., Ovens, D., Steed, R., MacIver, M., Grimit, E., Eckel, T., Lamb, B., Vaughan, J., Westrick, K., Storck, P., Colman, B., Hill, C., Maykut, N., Gilroy, M., Ferguson, S. A., Yetter, J., Sierchio, J. M., Bowman, C., Stender, R., Wilson, R., and Brown, W.: Regional environmental prediction over the Pacific Northwest, B. Am. Meteorol. Soc., 84, 1353–1366, 2003.
Napelenok, S. L., Pinder, R. W., Gilliland, A. B., and Martin, R. V.: A method for evaluating spatially-resolved NO_x emissions using Kalman filter inversion, direct sensitivities, and space-based NO_2 observations, Atmos. Chem. Phys., 8, 5603–5614, 2008, http://www.atmos-chem-phys.net/8/5603/2008/.
Parrish, D.: Critical evaluation of US on-road vehicle emission inventories, Atmos. Environ., 40,

2288–2300, 2006.

Pollack, A. K., Lindhjem C., Stoeckenius, T. E., Tran, C., Mansell, G., Jimenez, M., Wilson, G., and Coulter-Burke, S.: Evaluation of the US EPA MOBILE6 Highway Vehicle Emission Factor Model, ENVIRON International Corporation, www.epa.gov/OMS/models/mobile6/crce64.pdf, 2004.

Schaub, D., Boersma, K. F., Kaiser, J. W., Weiss, A. K., Folini, D., Eskes, H. J., and Buchmann, B.: Comparison of GOME tropospheric NO_2 columns with NO_2 profiles deduced from ground-based in situ measurements, Atmos. Chem. Phys., 6, 3211–3229, 2006, http://www.atmos-chem-phys.net/6/3211/2006/.

Tang, T., Roberts, M., Ho, C.: Sensitivity Analysis of MOBILE6 Motor Vehicle Emission Factor Model, US Department of Transportation, Federal Highway Administration, http://www.fhwa.dot.gov/resourcecenter/teams/airquality/mobile6_v2.pdf, 2002.

Zhao, C. and Wang, Y.: Assimilated inversion of NO_x emissions over east Asia using OMI NO_2 column measurements, Geophys. Res. Lett., 36, L06805, doi:10.1029/2008GL037123, 2009.

Zubrow, A., Chen, L., and Kotamarthi, V. R.: EAKF-CMAQ: Introduction and evaluation of a data assimilation for CMAQ based on the ensemble adjustment Kalman filter, J. Geophys. Res., 113, D09302, doi:10.1029/2007JD009267, 2008.

Table 1. Linear correlation and best fit slope of AIRPACT-3 to OMI tropospheric NO_2 column monthly averages for the entire domain. Corresponding areas where both KNMI and NASA showed the same trend relative to AIRPACT are noted.

		AIRPACT to KNMI slope	AIRPACT to KNMI *R*	AIRPACT to NASA slope	AIRPACT to NASA *R*	Corresponding trends
2007	Mar	0.36	0.593	0.98	0.715	Higher AIRPACT values in I-5 Corridor from Portland to Seattle. Higher OMI values in Victoria and surrounding Vancouver.
2007	Apr	0.52	0.636	0.81	0.769	Higher AIRPACT values in Seattle. Higher OMI values in Victoria and Vancouver.
2007	May	0.72	0.715	0.80	0.728	Higher AIRPACT values in I-5 corridor from Portland to Seattle. Higher OMI values in Salt Lake, Victoria, and Vancouver
2007	Jun	0.78	0.682	0.83	0.806	Higher AIRPACT values in Seattle and Portland. Higher OMI values in Salt Lake, Victoria, Vancouver, and central Washington.
2007	Jul	0.32	0.190	0.74	0.406	Much higher AIRPACT values in fire areas and higher values in Seattle. Higher OMI values in Vancouver, Salt Lake, north NV, and south ID.
2007	Aug	1.74	0.120	1.87	0.214	Much higher AIRPACT values in fire areas. Higher OMI values in Vancouver and Salt Lake.
2007	Sep	−0.50	−0.066	0.00	0.000	Much higher AIRPACT values in fire areas. Higher OMI values in Vancouver and central Washington
2007	Oct	0.10	0.047	0.31	0.113	Much higher AIRPACT values in fire areas. Higher AIRPACT values in Seattle. Higher OMI values in Vancouver.
2007	Nov	0.38	0.671	0.99	0.834	Higher AIRPACT values in Seattle and Boise. Higher OMI values in Vancouver
2007	Dec	0.19	0.380	0.66	0.729	Higher AIRPACT values over Washington, Montana, and Idaho. Higher OMI values in greater Calgary and Vancouver.
2008	Jan	0.31	0.626	0.92	0.840	Higher AIRPACT values in Washington and Portland. Higher OMI values in Victoria.
2008	Feb	0.35	0.680	1.10	0.868	Higher AIRPACT values in the Rockies, especially Boise and Spokane. Higher OMI values in Canadian waters.
2008	Mar	0.39	0.619	0.68	0.678	Higher AIRPACT values in Seattle. Higher OMI values in Victoria, Vancouver, and Tri-Cities
2008	Apr	0.68	0.715	0.68	0.735	Higher AIRPACT values in Seattle. Higher OMI values in central Washington, Victoria, and Vancouver.
2008	May	0.86	0.672	0.74	0.574	Higher AIRPACT values in I-5 Corridor from Portland to Seattle. Higher OMI values in Victoria and central Washington.
2008	Jun	1.01	0.727	0.90	0.747	Higher AIRPACT values in Seattle and Portland. Higher OMI values in Victoria and Vancouver.
2008	Jul	2.16	0.277	1.82	0.306	Much higher AIRPACT values over fires. Higher AIRPACT values in Seattle and Portland. Higher OMI values in Vancouver
2008	Aug	1.06	0.191	0.71	0.191	Much higher AIRPACT values over CA fires. Higher AIRPACT values in Seattle. Higher OMI values in Salt Lake and ID/NV/UT fire.

ACPD
9, 27063–27098, 2009

Table 2. Linear correlation and best fit slope of KNMI to NASA OMI tropospheric NO_2 column monthly averages for the analyzed domain. General bias trends are noted.

		KNMI to NASA slope	*R*	General trend comments
2007	Mar	1.41	0.627	Higher NASA values over coastal waters. Higher KNMI values in Salt Lake and I-5 corridor from Portland to Seattle.
2007	Apr	0.91	0.704	Higher NASA values over I-5 in Oregon, Spokane, and Boise. Higher KNMI values in western Washington and Salt Lake.
2007	May	0.83	0.758	Higher NASA values or no bias over most of the domain.
2007	Jun	0.68	0.755	Higher NASA values over most of the domain. Higher KNMI values in the Cascades and Salt Lake.
2007	Jul	0.65	0.601	Higher NASA values over most urban areas in the domain. Higher KNMI values in Salt Lake.
2007	Aug	0.46	0.773	Higher NASA values or no bias over the entire domain.
2007	Sep	0.57	0.794	Higher NASA values or no bias over the entire domain.
2007	Oct	0.61	0.476	Higher NASA values over northern part of domain. Higher KNMI values in Salt Lake and central Washington.
2007	Nov	1.50	0.725	Higher KNMI values in Salt Lake, Washington, Vancouver, and Victoria. Higher NASA values in B.C., Idaho, and Montana.
2007	Dec	0.63	0.348	Higher NASA values over coastal waters, western Oregon, Vancouver, Victoria, and the Rockies. Higher KNMI values surrounding Salt Lake.
2008	Jan	1.52	0.690	Higher NASA values over coastal waters, Portland, and the Rockies. Higher KNMI values over Salt Lake, Washington I-5, Victoria, and Vancouver
2008	Feb	1.70	0.721	Higher KNMI values in Salt Lake, western Washington, and western BC.
2008	Mar	0.91	0.582	Higher NASA values over water and I-5 in Oregon. Higher KNMI values in Salt Lake, west Washington, and Victoria.
2008	Apr	0.71	0.733	Higher NASA values over water, Western Oregon, Eastern Washington, and Boise. Higher KNMI values in Salt Lake.
2008	May	0.69	0.688	Higher NASA values over most of the domain. Higher KNMI values in the Cascades.
2008	Jun	0.68	0.780	Higher NASA values over most of the domain.
2008	Jul	0.50	0.661	Higher NASA values over most of the domain. Higher KNMI values in Salt Lake.
2008	Aug	0.49	0.728	Higher NASA values or no bias over the entire domain.

ACPD
9, 27063–27098, 2009

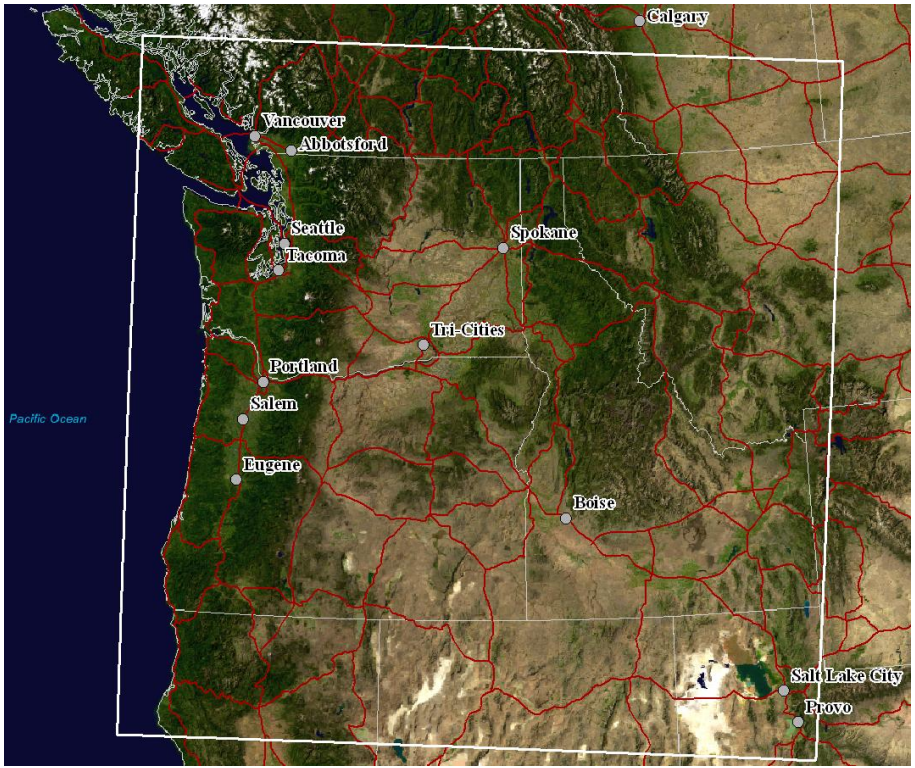

Fig. 1. The AIRPACT-3 domain. Satellite imagery of the AIRPACT-3 domain is shown with major highways in red.

ACPD

9, 27063–27098, 2009

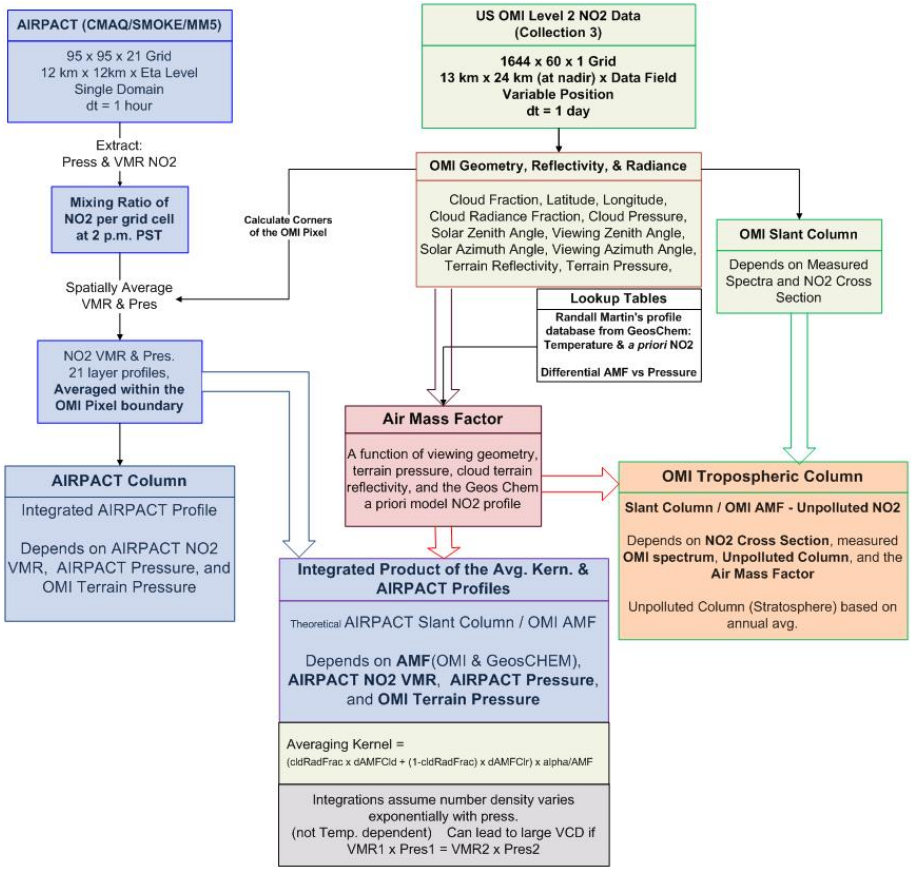

Fig. 2. Data flow for column comparisons using the averaging kernel.

ACPD
9, 27063–27098, 2009

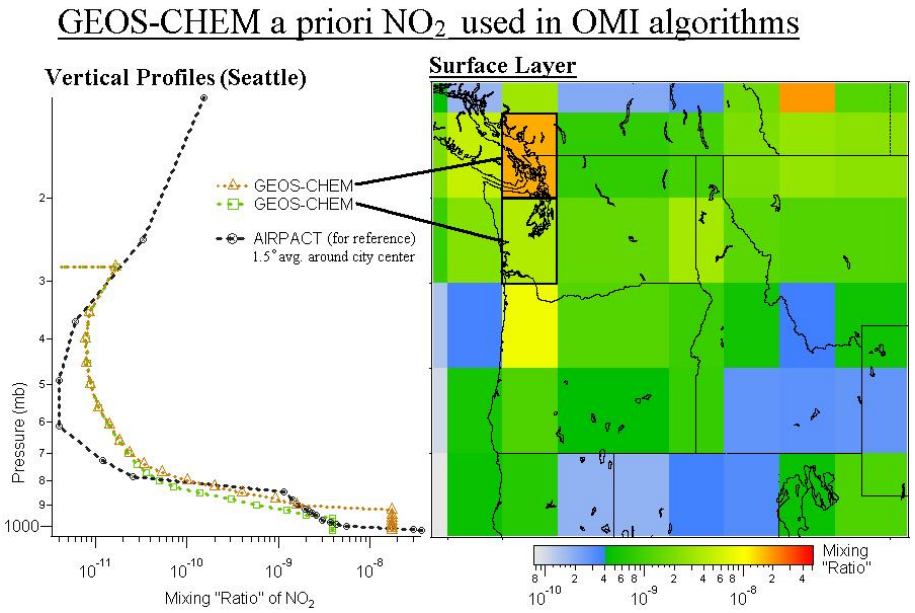

Fig. 3. A priori NO_2 used in OMI algorithms, developed by Randall Martin with GEOS-CHEM simulations. The grid below is a 2°×2° matrix used for the OMI (NASA) algorithm, regridded from the original GEOS-CHEM simulations with original resolution of 2°×2.5°. Note the two pixels over the Seattle metro area with nearly an order of magnitude difference at the surface layer.

ACPD
9, 27063–27098, 2009

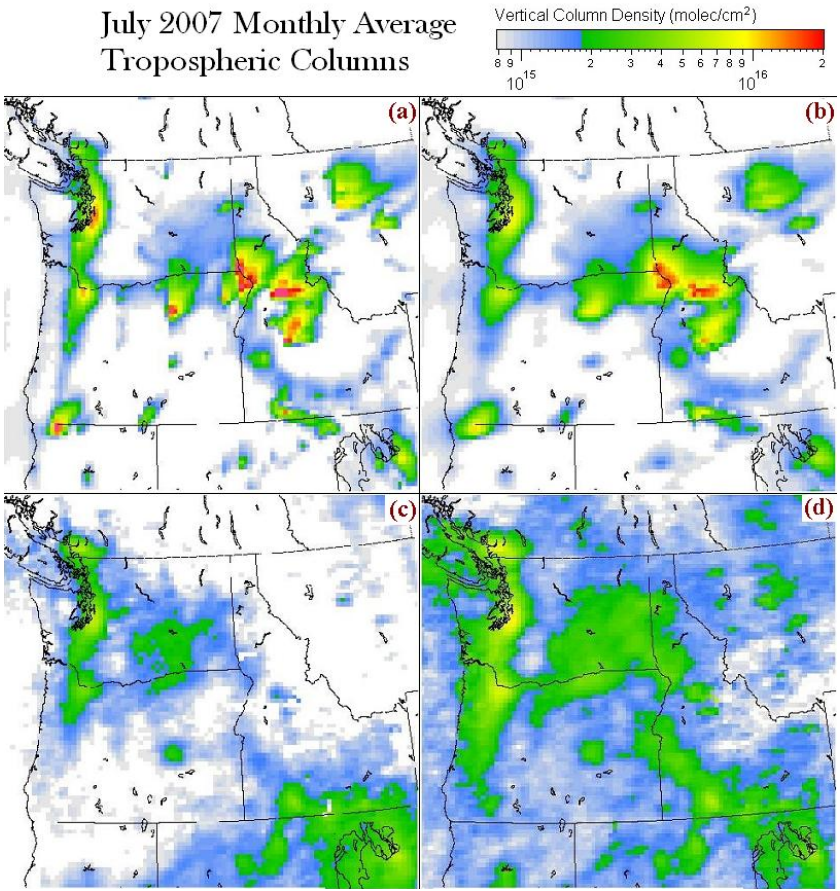

Fig. 4. Average tropospheric NO_2 columns are shown for the month of July 2007: AIRPACT **(a)** at upper left, spatially averaged AIRPACT **(b)** at upper right, KNMI OMI **(c)** at lower left, and NASA OMI **(d)** at lower right.

ACPD
9, 27063–27098, 2009

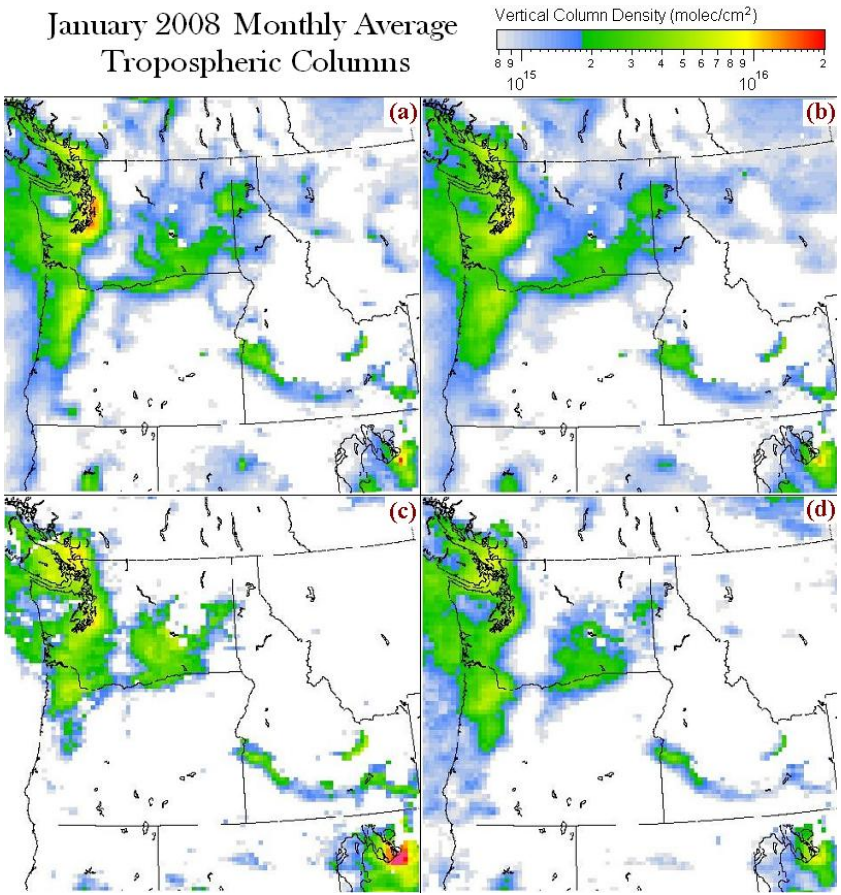

Fig. 5. Average tropospheric NO_2 columns are shown for the month of January 2008: AIRPACT **(a)** at upper left, spatially averaged AIRPACT **(b)** at upper right, KNMI OMI **(c)** at lower left, and NASA OMI **(d)** at lower right.

ACPD
9, 27063–27098, 2009

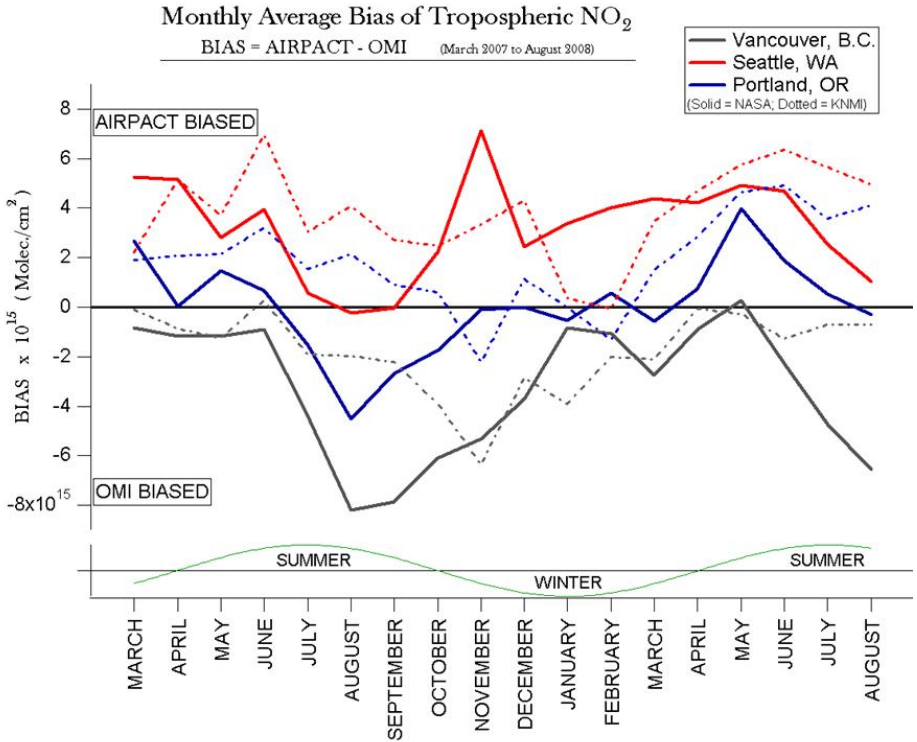

Fig. 6. Monthly average AIRPACT (spatially averaged) minus OMI, tropospheric NO_2 column biases in urban areas along the Interstate-5 Freeway from March 2007 to August 2008. Solid lines show NASA bias and dotted lines show KNMI bias. See Figs. 8, 10, and 12 for corresponding total tropospheric columns.

ACPD
9, 27063–27098, 2009

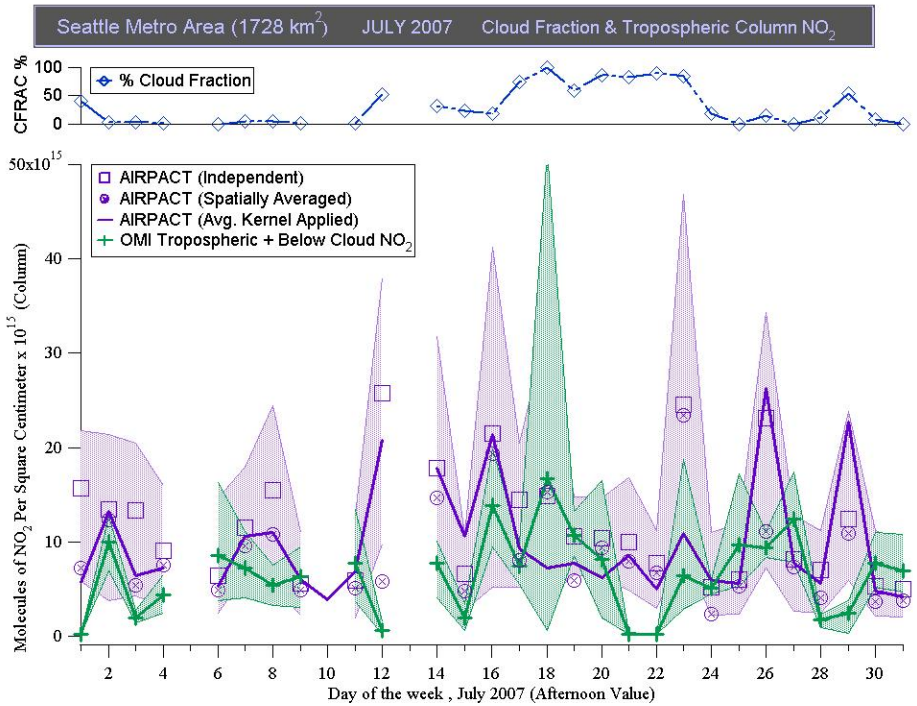

Fig. 7. Seattle metro area tropospheric NO_2 for July 2007 over a 1728 km^2 area (12 AIRPACT pixels). Maximum and minimum values over the averaged area are shown (shaded) for reference, as well as cloud fraction.

ACPD
9, 27063–27098, 2009

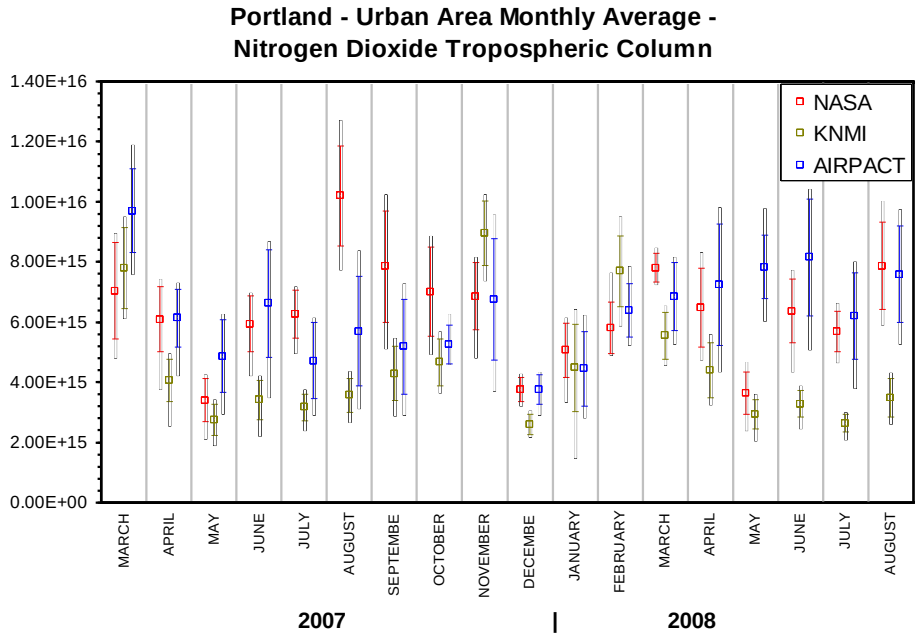

Fig. 8. Monthly average NO_2 for Portland, Oregon over 18 months. The bars show standard deviation of spatial variation over a 1152 km^2 area (8 AIRPACT pixels) while the whiskers show the extent of the maximum and minimum. Values are in molecules per square centimeter.

ACPD
9, 27063–27098, 2009

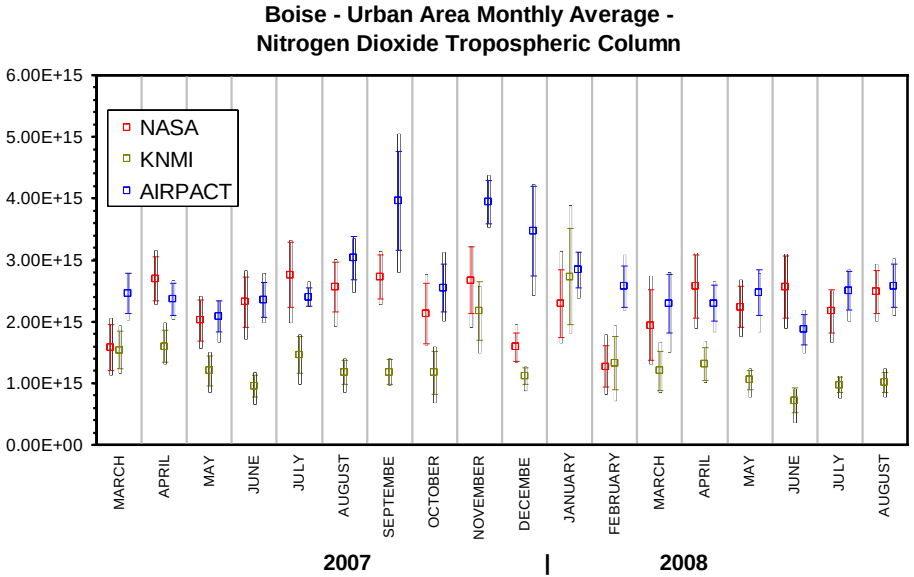

Fig. 9. Monthly average NO_2 for Boise, Idaho over 18 months. The bars show standard deviation of spatial variation over a 720 km^2 area (5 AIRPACT pixels) while the whiskers show the extent of the maximum and minimum. Values are in molecules per square centimeter.

ACPD
9, 27063–27098, 2009

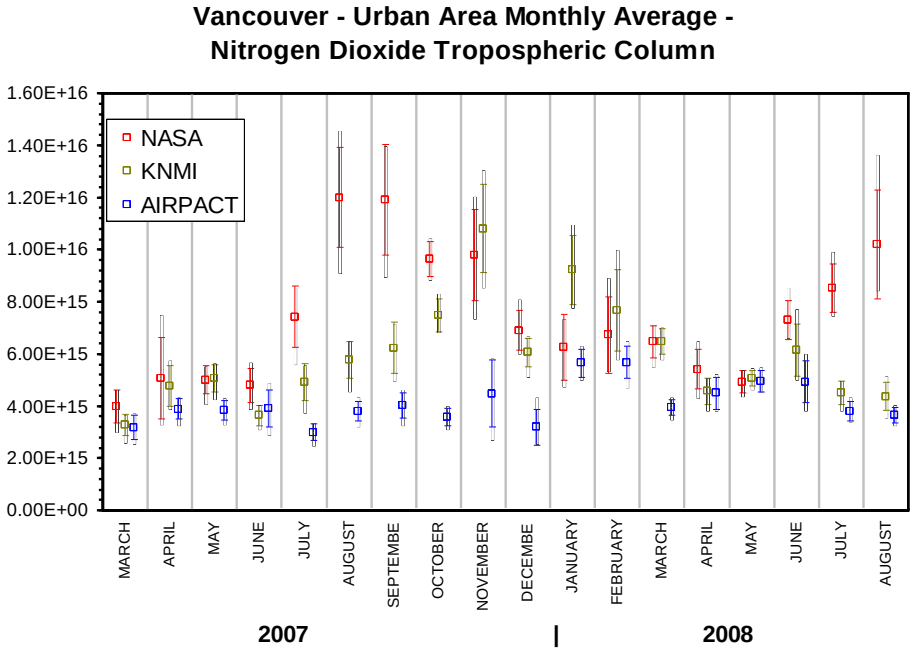

Fig. 10. Monthly average NO_2 for Vancouver, British Columbia over 18 months. The bars show standard deviation of spatial variation over a 720 km^2 area (5 AIRPACT pixels) while the whiskers show the extent of the maximum and minimum. Values are in molecules per square centimeter.

ACPD
9, 27063–27098, 2009

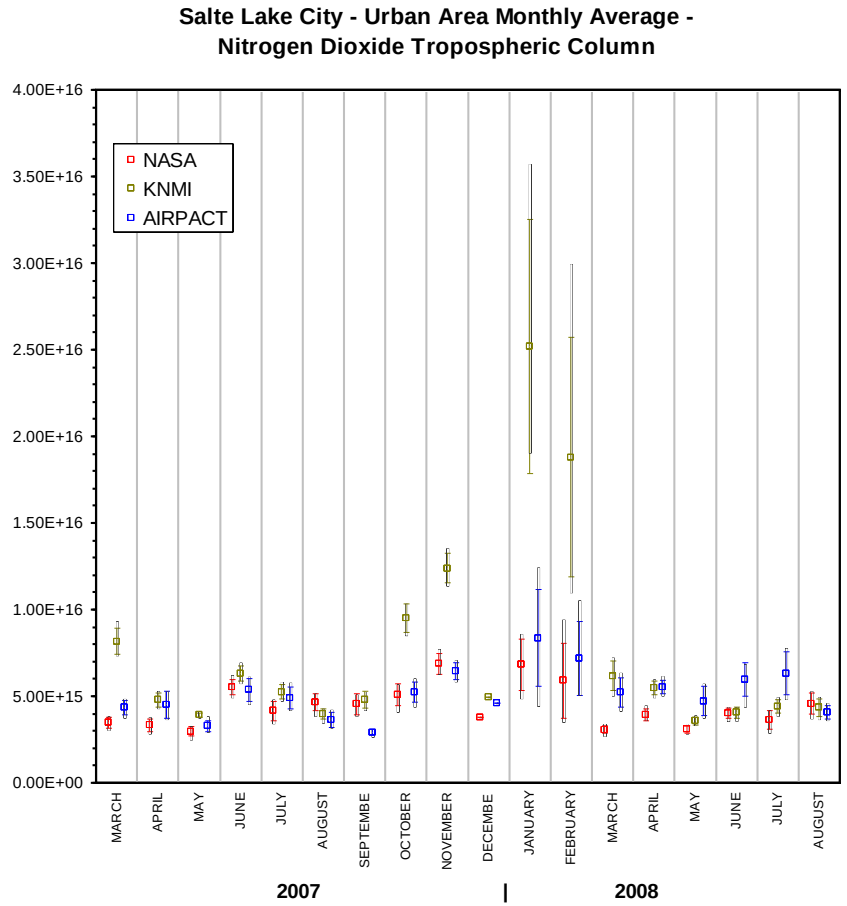

Fig. 11. Monthly average NO_2 for Salt Lake City, Utah over 18 months. The bars show standard deviation of spatial variation over a 720 km^2 area (5 AIRPACT pixels) while the whiskers show the extent of the maximum and minimum. Values are in molecules per square centimeter.

ACPD
9, 27063–27098, 2009

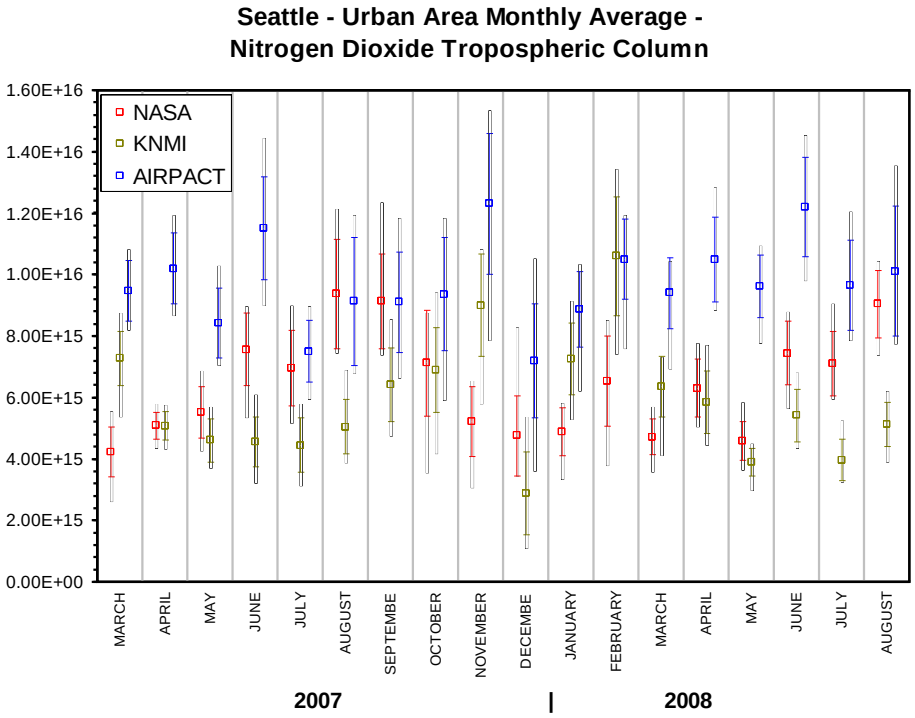

Fig. 12. Monthly average NO_2 for Seattle, Washington over 18 months. The bars show standard deviation of spatial variation over a 1728 km^2 area (12 AIRPACT pixels) while the whiskers show the extent of the maximum and minimum. Values are in molecules per square centimeter.

ACPD
9, 27063–27098, 2009